JOURNAL OF NANO- AND ELECTRONIC PHYSICS
Vol. 8 No 4(2), 04067(4pp) (2016)
ЖУРНАЛ НАНО- ТА ЕЛЕКТРОННОЇ ФІЗИКИ
Том 8 № 4(2), 04067(4cc) (2016)

Investigation of Nanostructure Phase Composition and Field Emission Properties in the Ge/Si(100) System

S.A. Nepijko[1,2], A.A. Sapozhnik[1], A.G. Naumovets[3], Yu.N. Kozyrev[3,4], M. Klimenkov[5], S.I. Protsenko[2], L.V. Odnodvorets[2], I.Yu. Protsenko[2]

[1] *Institute of Physics, University of Mainz, 7, Staudingerweg, 55128 Mainz, Germany*
[2] *Sumy State University, 2, Rymskyi-Korsakov Str., 40007 Sumy, Ukraine*
[3] *Institute of Physics, National Academy of Sciences of Ukraine, 46, Nauky Prosp., 03028 Kyiv, Ukraine*
[4] *Institute of Surface Chemistry, National Academy of Sciences of Ukraine, 17, General Naumov Str., 03164 Kiev, Ukraine*
[5] *Institute for Applied Materials, Karlsruhe Institute of Technology, Hermann-von-Helmholtz-Platz 1, 76344 Eggenstein-Leopoldshafen, Germany*

(Received 25 November 2016; published online 23 December 2016)

We analyzed the Ge/Si(100) phase composition based on existing literature data and results obtained with high-resolution electron microscopy method. The research confirms formation of solid solutions Ge(Si) in the Ge film and the Si(Ge) in the Si (100) substrate, which are separated by a thin pseudomorphic layer. This conclusion can correctly interpret the phase composition of the heterostructure based on Ge and Si. An array of tips developing on the interface with the tip density of the order 10^{14} m^{-2} was visualized. The emission properties of the tips were studied, including electric field strength near their peaks reaching 10^9 V/m, which causes cold emission.

Keywords: Heterostructures, Phase Composition, Solid Solution, Pseudomorphic layers, Emission Properties.

DOI: 10.21272/jnep.8(4(2)).04067 PACS numbers: 73.22. – f; 73.21.La; 81.15.Hi

1. INTRODUCTION

A high interest in the nanostructures realized in bulk Ge and Si [1], thin Ge films grown on Si(111) [2, 3] and Si (100) [4] as well as multilayers Ge(1 nm)/Si(3 nm)]$_{25}$/Si(100) [5] or [Si(15 nm)/Ge(20 nm)]$_n$/Si (n = 2, 4 and 6) [6] is motivated by their high functionality and a broad spectrum of possible applications in electronics and photonics. In particular, field electron emission from bulk Ge and Si [1] or from Ge islands [2] and quantum dots (QD) [4] as well as their thermoelectric [5, 7] and photovoltaic [6] properties are considered to be of a great technological importance. An extensive study was also conducted on the thermodynamic properties [8], diffusion processes [9], the mechanisms and the stability temperature intervals for 2D-growth process of Ge films on Si with formation of hut, dome and superdome clusters [3,10,11]. Heteroepitaxial growth of Ge on Si(100) was analyzed in Ref. [12].

The thermodynamic relation $E_1 \geq E_2 + E_{12} + E_g(d)$ was employed, where E_1, E_2 and E_{12} are the free energy of the substrate, the film, and the interface between them, and E_g is the film deformation energy depending on the film thickness d. The conclusion has been made that Frank-van der Merwe (FvdM) mechanism is realized at the initial stages of condensation, which changes to Volmer-Weber (VW) mechanism at the later stages. The reason for that is relaxation of elastic deformations in Ge islands via formation of misfit dislocations. Calculation of the elastic deformation spatial distribution during formation of a QD in a Ge/Si(100) system showed that a QD is expanded in the growth direction and contracted in the perpendicular direction [13]. At the same time, the region close to the top of a QD appears to be mostly relaxed.

Investigation of nanostructures at the interface between Ge and Si with high resolution transmission electron microscopy (HRTEM) turned out to be very informative [10, 11]. For example, it allowed to scrutinize formation of small and large *dome* QD [10]. It was shown that the phase diagram of a Si-Ge system is cigar-shaped and characterized by formation of a continuous sequence of solid solutions (SS) for all concentration ratios [9]. SS forms at both sides of the interface between a Ge layer and a Si single crystal substrate, since the diffusion coefficients and the activation energies of both materials have close values [9, 14, 15]. Presence of a natural oxide on the surface of a Si substrate doesn't significantly influence these parameters [15]. Investigating the magnetic properties of Mn doped QD in a Ge/Si(100) system revealed anomalous diffusion of Si atoms from the substrate into Ge QDs in this magnetic semiconductor [11].

2. EXPERIMENTAL PROCEDURE

The Ge/Si(100) heterostructures were prepared by the molecular-beam epitaxy (MBE) method. At epitaxial growth of Ge on Si, mechanical strains develops which are caused by 4.2 % difference in the lattice constants. The mechanical strain is partially compensated due to formation of SS pseudomorphic layers Ge(Si) in Ge and Si(Ge) in Si. In order to provide an atom mobility necessary for driving the system to the thermodynamic equilibrium, the growth temperature was maintained at a value of 600-1000 K. In-situ control of the crystal structure and the chemical composition was realized with the reflection high-energy electron diffraction (RHEED) and Auger-spectroscopy.

Electron emission studies were performed in a diode

 © 2016 Sumy State University

cell mounted in a ultra-high vacuum (UHV) chamber. The pressure in the chamber was less than 3×10^{-11} mbar. After these measurements, the sample was prepared according to the method described in Ref. [16] for investigations in a Philips 300 CM transmission electron microscope with a LaB_6 cathode (the accelerating voltage was 300 kV, the line resolution was 0.14 nm). The high-resolution transmission electron microscopy (HRTEM), the bright- and dark-field including the high-angle annular dark field (HAADF) methods, as well as the electron diffraction were applied in this study. An area from which the electron diffraction was normally observed approached 1 μm in diameter.

3. RESULTS AND DISCUSSION

The bright-, dark-field, and HAADF operational modes of a transmission electron microscope proide the same information, however, a deeper contrast is realized in the last case. It is important while studying week-contrast systems, which is illustrated by the HAADF image of a Ge/Si(100) heterostructure shown in Fig. 1. In this case, the thickness d of the epitaxially grown layer is 8.7 nm $\simeq 32a_{200} = 16\ a_{100}$ (the Si lattice parameter $a_{100} = 0.54307$ nm). The mechanically strained region exhibits a darker contrast. In Fig. 1, it propagates from the (100) surface to the bulk of the crystal reaching a depth ~10 μm.

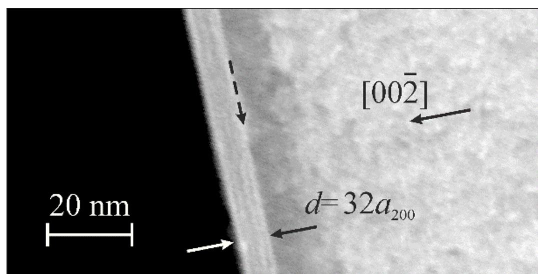

Fig. 1 – HAADF image of a Ge/Si(100) heterostructure cross-section. The dashed arrow marks the interface between the epitaxially grown layer and the Si single crystal substrate

The HRTEM images of the Ge/Si(100) heterostructure are shown in Fig. 2a. The detailed images of the regions marked with the white squares are given in Fig. 2b and c. The epitaxial layer is represented in Fig. 2b and the Si single crystal is shown in Fig. 2c. Atomic plane fringes of (200) and (111) types are distinctly visible in both figures.

Fast Fourier transforms (FFT) of Fig. 2b and c are given in Fig 2b' and c' respectively. They illustrate epitaxial character of the investigated Ge/Si(100) heterostructures. The epitaxial layer has the same crystal structure and a similar lattice parameter to the Si single crystal. The resolution of the method used is not enough for detecting the difference in the lattice parameters, however, two phases are surely present in the system (see also Refs. [9, 14, 15]). The spots in Fig. 2c correspond to strokes in Fig. 2b. These strokes are elongated in the direction perpendicular to the surface. It is explained by the fact that in the first case the phase corresponds to a volume with large linear dimensions, while in the second case the phase belongs to the epitaxially grown layer confined in the perpendicular direction.

A region of the Ge/Si(100) heterostructure having no crystal structure defects and roughnesses was favorable for FFT analysis. The area shown in Fig. 2a meets these requirements. The surface opposite to the interface of the epitaxially grown layer has defects, which represent itself tip-like nanostructures. Fig. 2a shows a part of the sample between such tips.

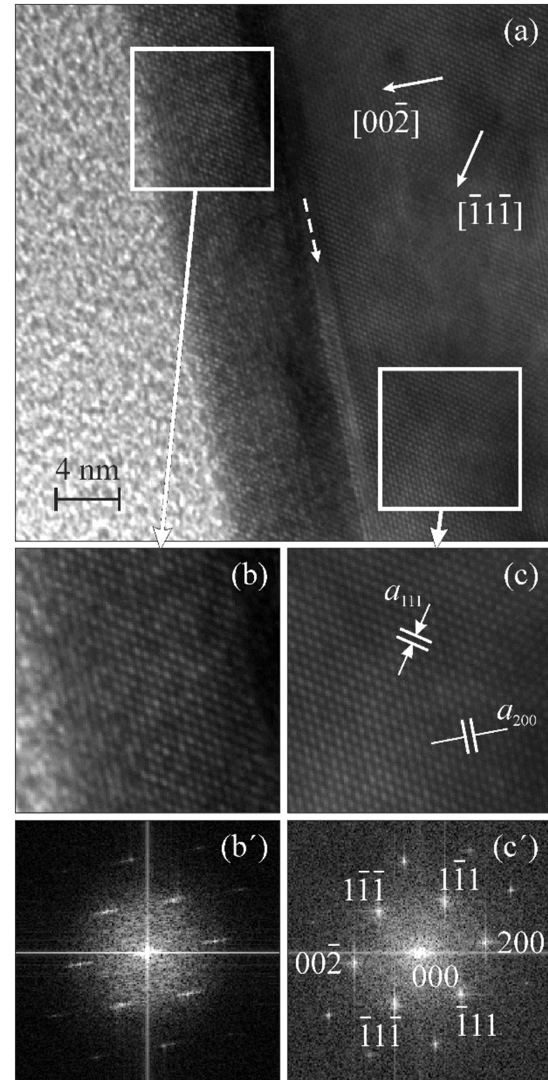

Fig. 2 – HRTEM images of a Ge/Si(100) heterostrusture cross-section (a). Detailed images of the regions marked with the white squares within the epitaxially grown layer (b) and the Si single crystal (c). FFT of the regions shown in (b) and (c) are represented in (b´) and (c´), respectively

A characteristic tip-like defect is illustrated in Fig. 3a. The region marked with the white square is represented in detail in the inset (Fig. 3b). The fringes representing the (200) type atomic planes are distinctly visible. The distance between these fringes in known from the literature to be $a_{200} = a_{100}/2 =$ 0.2715 nm. It allows to define the radius of a tip with a good precision. It is ~0.5 nm in this case. The values of the tip radii were distributed within 0.5-1.4 nm.

A fragment of the Ge/Si(100) heterostructure containing several tips is shown in Fig. 4a. The average distance between the tips estimated from this image is ~ 60 nm. Thus, the tip density is $\sim 3 \times 10^{-4}$ nm^{-2} $= 3 \times 10^{14}$ m^{-2}. A

more detailed image of the tip marked with the white square is given in the inset (Fig. 4b). Atomic plane fringes of (111) type are resolved in this case (Fig. 4b).

The emission properties of the investigated heterostructures are of a great interest. After applying a voltage of several volts to a collector with a curvature radius of the order of 1 nm, electric field can reach values

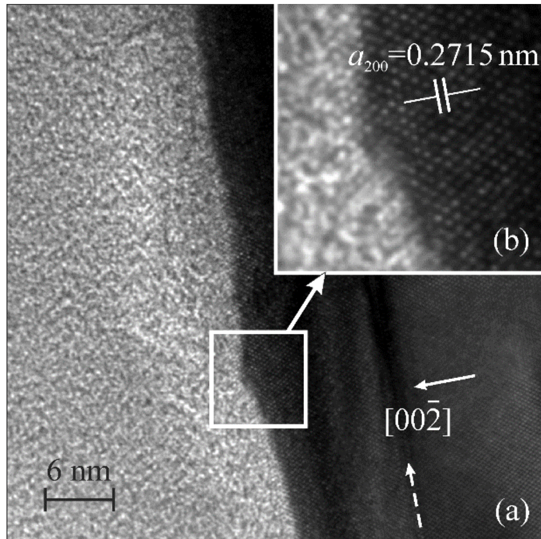

Fig. 3 – HRTEM images of a Ge/Si(100) heterostructure cross-section with a tip having a curvature radius of 0.5 nm (a). A detailed image of the tip with distinctly visualized atomic plane fringes of (200) type (b)

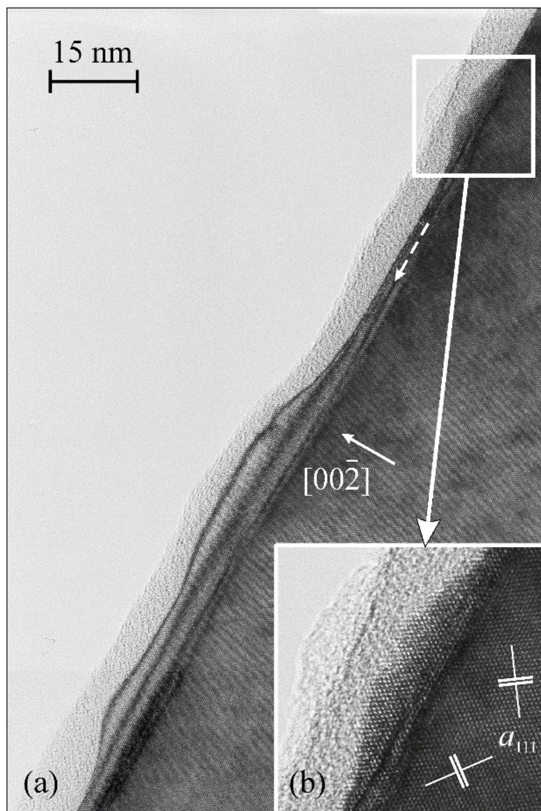

Fig. 4 – To calculation of the tip concentration in the investigated Ge/Si(100) heterostructure (a). A detailed image of a tip with distinctly visualized atomic plane fringes of (111) type (b)

> 10^7 V/cm. These values are enough for achieving field electron emission. The current-voltage characteristic (*I-U* curve) of the investigated Ge/Si(100) heterostructure is shown in Fig. 5. The measurements were performed at room temperature, the photocurrent reached 1 mA/cm^2 and was homogeneous across the surface. The *I-U* curve is not monotonous, it exhibits several local maxima. This behavior of the current-voltage characteristic

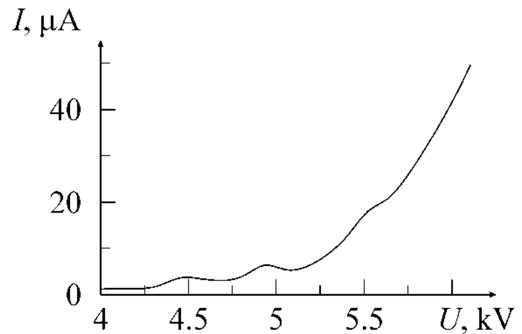

Fig. 5 – The field electron emisson *I-U* curve of the Ge/Si(100) heterostructure having tips at the interface

can be explained by electron energy quantization in tips having hut, dome and superdome shapes in a Ge/Si(100) heteorstructure In our case, a quantum well forms in the interfacial region between Si and Ge [4]. Its depth is defined primarily by the bandgap widths in Ge and Si. An external electric field is enhanced close to a tip and, penetrating into the tip, induces a shift of the energy levels. When the vacuum level coincides with an energy level in the quantum well, electrons tunnel resonantly to vacuum. This process is indicated with a peak at the current-voltage characteristic curve. An estimation of the emission properties taking into account the real energy structure of a Ge/Si(100) heterojunction is presented in Ref. [17].

4. CONCLUSIONS

Studying the structure and emission properties of nanostructures formed at the interface between a Si(100) substrate and a Ge layer grown on it with MBE technique indicates that two coupling mechanisms FvdM and VW are implemented sequentially during the deposition process. As Ge and Si atoms exhibit unrestricted mutual solubility, conclusion can be made that mutual diffusion of atoms takes place already during condensation of Ge atoms onto a Si(100) with or without a natural oxide layer. It leads to SS formation, namely Ge(Si) in Ge and Si(Ge) in Si. Similar values of the diffusion coefficients and activation energies lead to mixing Ge and Si atoms [9, 14, 15]. A very thin pseudomorphic layer forms at the interface due to an inconsistency of Ge and Si lattice parameters. Thus, it can be assumed that the emission properties of epitaxially prepared Ge/Si(100) system (see, e.g. Refs. [2-4]), are relevant to the islands/QD, which consist not of pure Ge, but a SS bases on it. Our study clarify the phase composition of nanostructures in such systems. Studying field emission from Ge/Si(100) heterostructures, having a non-monotonous character, is of a high interest for creating nanoelectronic devices based on new operational principles.

ACKNOWLEDGEMENTS

One of the authors (S.A.N.) expresses his sincere gratitude to G. Ertl for interest in the work and discussing the results.

REFERENCES

1. F.G. Allen, *J. Phys. Chem. Solids* **19**, 87 (1961).
2. V.N. Tondare, B.I. Birajdar, N. Pradeep, D.S. Joag, A. Lobo, S.K. Kulkarni, *Appl. Phys. Lett.* **77**, 2394 (2000).
3. A.I. Nikiforov, V.A. Cherepanov, O.P. Pchelyakov, *Semiconductors* **35**, 988 (2001).
4. A.A. Dadykin, Yu.N. Kozyrev, A.G. Naumovets, *JETP Letters* **76**, 472 (2002).
5. A. Matoba, H. Watase, M. Kitai, K. Sasaki, *Mater. Trans.* **49**, 1723 (2008).
6. S.A. Shan, A.F. Khan, A.U. Khan, *Appl. Surf. Sci.* **296**, 185 (2014).
7. J. Cheng, D. Agrawal, Y. Zhang, R. Roy, A.K. Santra, *J. Alloys Comp.* **491**, 517 (2010).
8. V.G. Deibuk, Yu.G. Korolyuk, *Semiconductor Physics. Quantum Electronics and Optoelectronics* **5**, 247 (2002).
9. S.L. Cui, L.J. Zhang, W.B. Zhang, Y. Du, H.H. Xu, *J. Min. Metall. Sect. B-Metall.* **48**, 227 (2012).
10. L. Wang, T. Liu, Q. Jia, Z. Zhang, D. Lin, Y. Chen, Y. Fan, Z. Zhong, X. Yang, J. Zou, *APL Materials* **4**, 040701 (2016).
11. J. Kassim, C. Nolph, M. Jamet, P. Reinke, J. Floro, *Appl. Phys. Lett.* **101**, 242407 (2012).
12. D.J. Eaglesham, M. Cerullo, *Phys. Rev. Lett.* **64**, 1943 (1990).
13. A.V. Dvurechenskii, A.I. Yakimov, *Semiconductors* **35**, 1095 (2001).
14. B.P. Uberuaga, M. Leskovar, A.P. Smith, H. Jónsson, M. Olmstead, *Phys. Rev. Lett.* **84**, 2441 (2000).
15. H.H. Silvestri, H. Bracht, J. Lundsgaard Hansen, A. Nylandsted Larsen, E.E. Haller, *Semicond. Sci. Technol.* **21**, 758 (2006).
16. O. Fedchenko, S.V. Chernov, M. Klimenkov, S.I. Protsenko, S.A. Nepijko, G. Schönhense, *Jpn. J. Appl. Phys.* **55**, 02BC15 (2016).
17. A.I. Yakimov, V.A. Markov, A.V. Dvurechenskii, O.P. Pchelyakov, *J. Phys. Condens. Matter.* **6**, 2573 (1994).